DOI: 10.1002/anie.201008004

Protein Engineering

Post-Crystal Engineering of Zinc-Substituted Myoglobin to Construct a Long-Lived Photoinduced Charge-Separation System**

Tomomi Koshiyama, Masanobu Shirai, Tatsuo Hikage, Hiroyasu Tabe, Koichiro Tanaka, Susumu Kitagawa, and Takafumi Ueno**

Photoinduced electron transfer (ET) in native photosynthesis reactions is efficiently achieved by the accumulation of different types of redox cofactors within protein assemblies immobilized in cell membranes.[1–3] The precise arrangement of each cofactor in the molecular spaces enables them to retain the long-lived charge-separated state, which promotes multistep reactions in biological systems. To elucidate the mechanism of the biological ET reactions and to develop light energy conversion systems, artificial ET proteins have been constructed using de novo proteins, chemical modification of native cofactors, photocatalytic reaction centers engineered into protein assemblies, and design of synthetic metal complexes immobilized in protein–protein ET systems.[4–12] The reported systems have provided insights into control of ET rates in terms of the distance between donors and acceptors, hydrogen-bonding interactions, reorganization energy of cofactors, and other factors.[4–12] Control of the dense accumulation of the different redox cofactors observed in natural photosystems required to achieve long-lived charge-separated state has caused difficulties in efforts to duplicate this process using artificial protein systems in solution.[13] Thus, the design of novel protein frameworks that allow construction of a dense array of various cofactors is a worthwhile goal.

Protein crystals can be regarded as excellent candidates for the development of artificial ET reaction systems because the crystal lattices are expected to allow different types of cofactors to be arranged in three-dimensional frameworks that mimic the native ET systems. ET reactions in single protein crystals have been investigated for the dependence of long-range ET on the structures and orientations of redox centers within proteins.[14–16] Gray et al. constructed photochemically-initiated protein–protein ET reactions in protein crystals containing zinc-substituted cytochrome *c* peroxidase or ruthenium-modified azurin.[14–16] Moreover, protein crystals provide nanosized spaces for the fixation of metal ions, metal complexes, and the diffusion of organic molecules.[17–22] For instance, accumulation of metal ions and metal complexes in a protein crystal lattice spaces was accomplished simply by soaking of the crystals in a solution containing their precursors.[17–19] Anisotropic diffusion of small molecules in hen egg-white lysozyme (HEWL) crystals has been investigated by experimental and simulation approaches.[21,22] The results suggest that these features are governed by steric repulsion and electrostatic interaction induced by amino acid residues located on the internal surface of the crystal lattices. Thus, if we can precisely arrange donor and acceptor molecules and mediators in protein crystals, it is expected that the novel three-dimensional framework will allow us to achieve a long-lived charge-separated state.

Herein, we construct an artificial long-lived photoinduced charge-separation system using a protein crystal with different redox cofactors fixed in defined locations. We demonstrate the photoinduced multistep ET in a sperm whale myoglobin (Mb) single crystal. Methyl viologen (MV)-mediated ET occurs in the crystal between zinc porphyrin (ZnP; electron donor) and an oxo-centered triruthenium cluster (Ru_3O; electron acceptor; Scheme 1). The Mb crystals with space group *P*6 form several channel structures (diameter 2–4 nm), which provide enough space for accumulation of nanosized functional molecules as previously reported.[24] The Mb crystal spaces are available for site-specific fixation of Ru_3O and anisotropic diffusion of MV. Moreover, fixation of zinc porphyrin units with a light-harvesting function in the Mb crystal is achieved by crystallization of zinc porphyrin substituted myoglobin (ZnMb). Our engineered Mb crystals, in which ZnP and Ru_3O clusters are fixed at specific sites and which allow MV molecules to diffuse, contribute to providing the extremely long half-life of the final charge-separated state ($ZnP^{\bullet+}$-Ru_3O^0), which is 2800 times longer than that of a previously reported model system in organic solution.[25] This

[*] Dr. T. Koshiyama, Dr. M. Shirai, Prof. Dr. K. Tanaka, Prof. Dr. S. Kitagawa, Prof. Dr. T. Ueno
Institute for Integrated Cell-Material Sciences (iCeMS)
Kyoto University
iCeMS Lab Funai Center, Kyoto University Katsura
Nishikyo-ku, Kyoto 615-8510 (Japan)
Fax: (+81) 75-383-2812
E-mail: kitagawa@icems.kyoto-u.ac.jp
taka@icems.kyoto-u.ac.jp

T. Hikage
High Intensity X-ray Diffraction Laboratory
Nagoya University (Japan)

Prof. Dr. T. Ueno
PRESTO (Japan) Science and Technology Agency (JST)
Honcho Kawaguchi, Saitama 332-0012 (Japan)

H. Tabe, Prof. Dr. S. Kitagawa
Department of Synthetic Chemistry and Biological Chemistry,
Graduate School of Engineering, Kyoto University
Katsura, Nishikyo-ku, Kyoto 615-8510 (Japan)

[**] We thank Dr. Y. Tokita (Sony Corporation) for suggestions, and the members of BL38B1 of SPring-8 for assistance during the diffraction data collection. A Grant-in-Aid for Scientific Research (Grant No. 18655054 for T.U.) was awarded from the Ministry of Education, Culture, Sports, Science and Technology (Japan), and PRESTO, JST. Synchrotron radiation experiments were conducted under the approval of 2008A1124 and 2009B1065 at SPring-8.

Supporting information for this article is available on the WWW under http://dx.doi.org/10.1002/anie.201008004.

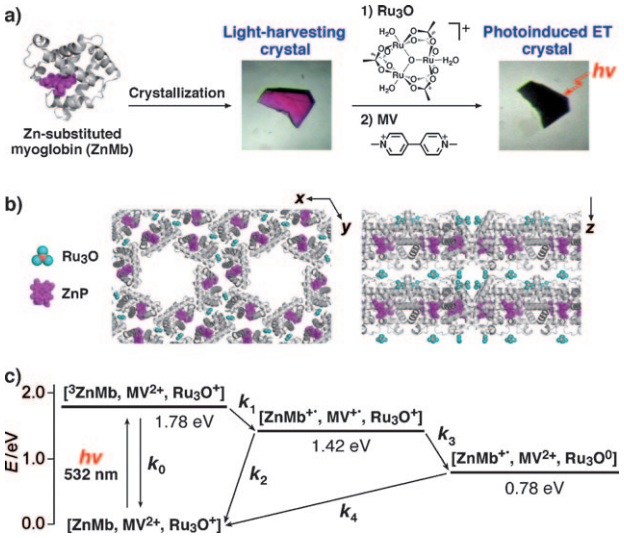

Scheme 1. a) Construction of a photoinduced electron transfer system in Mb crystals. b) Dense array of Ru_3O and ZnP in the ZnMb/Ru_3O crystal. c) Reaction and energy diagram for photoinduced electron transfer between ZnP and Ru_3O mediated by MV in a myoglobin crystal (see the Supporting Information).

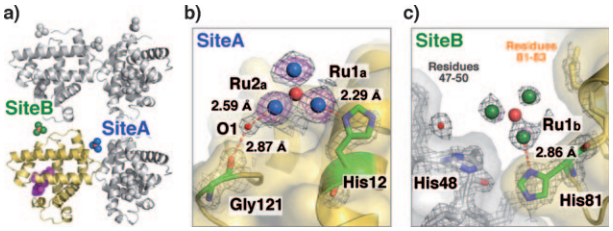

Figure 1. The structure of ZnMb/Ru_3O. a) Ru_3O binding sites in the crystal packing with the ZnMb monomer indicated by the yellow structure. The Ru atoms at SiteA, SiteB, and ZnP are colored blue, green, and magenta, respectively. b,c) The coordination structures of Ru_3O at SiteA (b) and SiteB (c) with anomalous difference Fourier maps of ruthenium atoms at 3.0σ (magenta), and the selected $2|F_O|-|F_C|$ electron-density maps at 1.0σ (gray). The oxygen atoms of Ru_3O and water molecules are shown as red spheres. In (c), amino acid residues of a neighboring Mb molecule are indicated by gray-colored tube models. These images were produced by Pymol.[23]

is the first example of an artificial ET system with a long-lived charge-separated state obtained by taking advantage of the characteristics of the three-dimensional space of protein crystals.

The site-specific fixation of ZnP was obtained by cofactor replacement and the site-specific fixation of Ru_3O was generated by crystal soaking. ZnMb was prepared according to a previously reported method.[26] The crystals were obtained under the conditions used to reconstitute Mb with monodepropionated heme.[27] To immobilize Ru_3O clusters in ZnMb crystals, the crystals were soaked in a buffer solution saturated with Ru_3O at 20 °C for 2 days. The absorption spectrum of the ZnMb/Ru_3O crystal has sharp peaks at 550 nm and 594 nm, which are assigned to the Q-band of ZnP, and a broad band at 680 nm that originates from the intracluster transition of Ru_3O moiety (Supporting Information, Figure S1).[28,29] The absorption intensities indicate that the ratio of ZnP to Ru_3O cluster is 1:1.3. The structure of the ZnMb/Ru_3O crystal was refined to a resolution of 1.75 Å with the space group *P*6 (PDB ID: 3ASE; Supporting Information, Table S1). The crystal structure indicates that the ZnMb monomer has two Ru_3O binding sites at His12 (SiteA) and His81 (SiteB), which are located in crevices formed by intermolecular associations within the crystal (Figure 1a). These crevices are essential for the fixation of the Ru_3O clusters because the Ru_3O clusters cannot bind to Mb in solution. This observation has been confirmed by ESI-TOF MS analysis (Supporting Information, Figure S2). Moreover, the Ru_3O binding structure at SiteA shows that the N^{ε} atom of His12 coordinates to the Ru1a atom with a bond length of 2.29 Å (Figure 1b). The Ru2a atom coordinates to a water molecule (O1; 2.59 Å), which is fixed by a hydrogen bond with the main-chain carbonyl of Gly121 (2.87 Å; Figure 1b). The Ru_3O cluster at SiteB is fixed in the space of a narrow crevice that is formed by intermolecular contact of residues 81–83 and residues 47–50 of a neighboring Mb molecule, with approximately 12 Å at the edges (Figure 1c). The Ru1b interacts weakly with the N^{ε} atom of His81 at a distance of 2.86 Å (Figure 1c). The occupancies of the ruthenium atoms at SiteA (0.8) are larger than those at SiteB (0.3) because Ru_3O at SiteA is stabilized by direct coordination with His12 and a water molecule. These results indicate that the site-specific fixation of Ru_3O clusters in the ZnMb/Ru_3O crystal is achieved by the coordination of the histidine residue and the hydrogen-bonding network in the crevice spaces combined with the intermolecular Mb–Mb association retaining the crystal lattice.

Photoinduced ET reactions in the single crystals were monitored by transient absorption spectroscopy at 298 K under an argon atmosphere. When a ZnMb crystal was excited at 532 nm, the excited-state (^{3}ZnMb) decay was observed and fitted to a monoexponential function with a rate constant of 75 s^{-1} (Supporting Information, Figure S3). This result indicated that the light-harvesting property of ZnMb in solution was maintained in the crystals because the rate was almost identical to that measured in solution.[26] Next, the ZnMb/Ru_3O crystal soaked in the buffer solution containing methyl viologen (MV) was found to exhibit electron transfer from ZnP to Ru_3O via the formation of $MV^{\bullet+}$ under the same conditions (Scheme 1, Figure 2; Supporting Information, Figure S4). Direct electron transfer from ^{3}ZnMb to Ru_3O^+ was not observed with the excitation at 532 nm in the ZnMb/Ru_3O crystal in the absence of MV. Thus, excitation of the MV-soaked ZnMb/Ru_3O crystal at 532 nm led to the prompt appearance of two absorption bands assigned to the methyl viologen cation radical ($MV^{\bullet+}$) and the ZnP π-radical cation ($ZnP^{\bullet+}$), which have marker bands at 610 nm and 670 nm, respectively (Figure 2a).[9] These species were generated via ^{3}ZnP (470 nm and 810 nm) as shown in the spectrum at 0.5 μs. The absorbance change of $MV^{\bullet+}$ in the early time scale ($t >$ 10 ns) was not extracted owing to overlap of it with the strong emission of ZnP in the crystal up to 40 ns (Supporting Information, Figure S4). The changes in the absorption spectrum that occur from 0.5 μs to 5 μs include the appearance of a new broad absorption band at around 880 nm, which

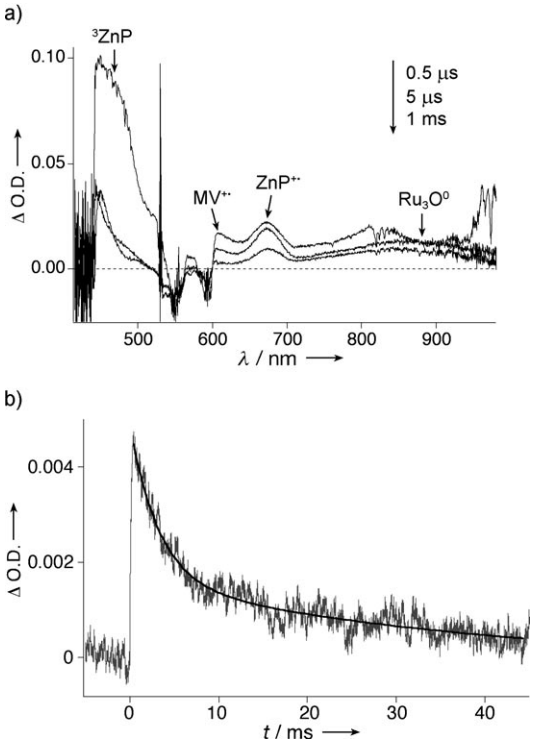

Figure 2. a) Difference absorption spectra observed after laser excitation ($\lambda = 532$ nm) of a MV-soaked ZnMb/Ru$_3$O crystal for the following delay times: 0.5 μs, 5 μs, 1 ms. b) Ru$_3$O^0 decay kinetically monitored at 880 nm. The change in optical density ΔO.D. is normalized.

was assigned to $[Ru_3(\mu_3\text{-}O)(\mu\text{-}CH_3COO)_6(H_2O)_3]^0$ (Ru_3O^0).[25,29] This change was accompanied by the decay of $MV^{+\bullet}$ at 610 nm. The final charge-separated state ($ZnP^{+\bullet}$ and Ru_3O^0 pair) was generated in the crystal up to 5 μs after the excitation according to the electron-transfer process shown in Scheme 1. The decay of Ru_3O^0 (880 nm) in the MV-soaked ZnMb/Ru$_3$O crystal is fit by a triexponential function that has three rate constants, 350 s^{-1} (0.06), 300 s^{-1} (0.58), and 24 s^{-1} (0.36). The lifetimes (τ) of the resulting charge-separated states were found to be 2.8 ms, 3.3 ms, and 41 ms, respectively (Figure 2b, values in parentheses represent each ratio of the kinetic phase).

The ET from $MV^{+\bullet}$ to Ru_3O^+, and the subsequent long-lived charge-separated state ($ZnP^{+\bullet}/Ru_3O^0$ of ZnMb/Ru$_3$O/MV) are only achieved in the crystal. The half-life values ($t_{1/2}$), which are calculated by $t_{1/2} = \tau \ln 2$ for 2.8 ms, 3.3 ms, and 41 ms, are 190, 220, and 2,800 times longer, respectively, than the values reported for zinc tetraphenylporphyrin/hexyl viologen/$[Ru_3(\mu_3\text{-}O)(\mu\text{-}CH_3COO)_6(4\text{-cyanopyridine})_3]^+$ system in acetonitrile ($t_{1/2} = 10$ μs).[25] Furthermore, ET from $MV^{+\bullet}$ to Ru_3O^+ was not observed in a buffer solution containing ZnMb, Ru$_3$O, and MV, because ESI-TOF MS measurements have confirmed that Ru$_3$O clusters cannot bind to Mb in solution (Supporting Information, Figure S2). Thus, it is expected that the fixation of ZnP and Ru$_3$O in the three-dimensional Mb crystal space allows 1) the close approach of MV molecules to ZnP and Ru$_3$O, 2) the small reorganization energy of the Ru$_3$O cluster, and 3) the spatial separation of $ZnP^{+\bullet}$ and Ru_3O^0 species.[30] The crystal structure of ZnMb/Ru$_3$O reveals that ZnP and Ru$_3$O are site-specifically located over intra- and interprotein contacts with separation distances of 21–23 Å (Figure 3a). On the other hand, although the unambiguous positions of MV

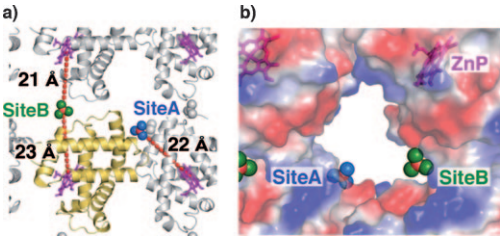

Figure 3. a) Separation distances between Ru$_3$O and ZnP in the crystal packing of ZnMb/Ru$_3$O. The ZnMb monomer is indicated by the yellow structure. b) Electrostatic potential of the fixation sites of Ru$_3$O and ZnP in the crystal. The surface is colored with a spectrum (ranging from red to blue for the negative to positive charge of each residue). These images were produced by Pymol.[23]

molecules were not determined by X-ray crystal structure analysis, positively charged MV molecules are expect to diffuse around ZnP and Ru$_3$O in the crystal because the negatively charged binding sites of ZnP and Ru$_3$O govern the diffusion of MV molecules in the crystal channels, as reported for the Cl^- ion/HEWL crystal system (Figure 3b).[21,22] It is suggested that the unique diffusion of MV in the crystal plays an essential role in mediating ET between ZnP and Ru$_3$O to extend charge separation, in contrast to the fixation of Trp122, which facilitates multistep electron tunneling, in an intramolecular Re-Trp-Cu(azurin) photosystem.[1,31] The fixation of Ru$_3$O clusters in the hydrophobic crevices is expected to decrease the reorganization energy of the Ru$_3$O cluster and allow rapid electron transfer of $MV^{+\bullet} \rightarrow Ru_3O^+$ and slow recombination of $ZnP^{+\bullet}/Ru_3O^0 \rightarrow ZnP/Ru_3O^+$ (Figure 1).[3,14,30] The lifetimes of the interprotein pathway at SiteB (21 Å) and at SiteA (22 Å) and the intraprotein pathway at SiteB (23 Å) were found to be 2.8 ms, 3.3 ms, and 41 ms, respectively, according to the distance between $ZnP^{+\bullet}$ and Ru_3O^0 in the crystal lattice (Figure 3a). The distance decay constant of these pathways ($\beta = 1.3$ $Å^{-1}$) is satisfied with the coupling zone of proteins reported by Gray et al.,[32] wherein the driving force and the reorganization energy of Ru$_3$O are assumed to be the same for SiteA and SiteB (see Supporting Information). Thus, we conclude that the appropriate arrangement of ZnP, Ru$_3$O, and MV molecules for the long-lived charge separation state is available in the three-dimensional crystal system but not in solution.

We have shown that the crystal space of Mb is ideal for creating an artificial ET reaction with a long-lived charge-separated state. We have demonstrated that ZnP, Ru$_3$O, and MV are accumulated in the three-dimensional crystal space of Mb by cofactor replacement, soaking, and diffusion, respectively. These processes of accumulation can only be carried out for the crystal, because the fixation is controlled by electrostatic interactions with the pore surface of the crystal, and the coordination of His residues/hydrogen-bonding network on the crevices formed by intermolecular association in

the Mb crystals. The crystal space allows the formation of the site-specific dense array with the small reorganization energy of the redox cofactors, as observed in native membrane proteins of photosynthesis. Consequently, we have succeeded in constructing a photoinduced artificial ET system and achieving a charge-separated state with a long half-life, which is up to 2800 times longer than that of the previously reported system in organic solution.[25]

In summary, this is the first example of a dense array of different cofactors enabling the formation of a long-lived charge-separated state in the artificial three-dimensional protein framework. This work reveals the importance of condensed molecular spaces of protein crystals for control of the spatial organization of different metal cofactors. Thus, our results may provide insights into the role of naturally occurring densely packed protein assemblies which mediate efficient ET reactions. Further efforts to design efficient ET reactions in protein crystals are in progress.

Received: December 18, 2010
Revised: February 14, 2011
Published online: April 14, 2011

Keywords: charge separation · electron transfer · hybrid materials · myoglobin · protein crystals

[1] J. L. Dempsey, J. R. Winkler, H. B. Gray, *Chem. Rev.* **2010**, *110*, 7024 – 7039.
[2] C. C. Page, C. C. Moser, X. X. Chen, P. L. Dutton, *Nature* **1999**, *402*, 47 – 52.
[3] *Biological Inorganic Chemistry-Structure & Reactivity* (Eds.: I. Bertini, H. B. Gray, E. I. Stiefel, J. S. Valentine), University Science Books, Herndon, **2007**.
[4] Z. X. Liang, I. V. Kurnikov, J. M. Nocek, A. G. Mauk, D. N. Beratan, B. M. Hoffman, *J. Am. Chem. Soc.* **2004**, *126*, 2785 – 2798.
[5] J. J. Wilker, I. J. Dmochowski, J. H. Dawson, J. R. Winkler, H. B. Gray, *Angew. Chem.* **1999**, *111*, 93 – 96; *Angew. Chem. Int. Ed.* **1999**, *38*, 89 – 92.
[6] B. Conlan, N. Cox, J. H. Su, W. Hillier, J. Messinger, W. Lubitz, P. L. Dutton, T. Wydrzynski, *Biochim. Biophys. Acta Bioenerg.* **2009**, *1787*, 1112 – 1121.
[7] T. Ueno, N. Yokoi, M. Unno, T. Matsui, Y. Tokita, M. Yamada, M. Ikeda-Saito, H. Nakajima, Y. Watanabe, *Proc. Natl. Acad. Sci. USA* **2006**, *103*, 9416 – 9421.
[8] T. Hayashi, Y. Hisaeda, *Acc. Chem. Res.* **2002**, *35*, 35 – 43.
[9] Y. Z. Hu, S. Tsukiji, S. Shinkai, S. Oishi, I. Hamachi, *J. Am. Chem. Soc.* **2000**, *122*, 241 – 253.
[10] C. Tommos, J. J. Skalicky, D. L. Pilloud, A. J. Wand, P. L. Dutton, *Biochemistry* **1999**, *38*, 9495 – 9507.
[11] J. W. Bryson, S. F. Betz, H. S. Lu, D. J. Suich, H. X. X. Zhou, K. T. Oneil, W. F. Degrado, *Science* **1995**, *270*, 935 – 941.
[12] I. Willner, E. Katz, *Angew. Chem.* **2000**, *112*, 1230 – 1269; *Angew. Chem. Int. Ed.* **2000**, *39*, 1180 – 1218.
[13] D. Noy, C. C. Moser, P. L. Dutton, *Biochim. Biophys. Acta Bioenerg.* **2006**, *1757*, 90 – 105.
[14] B. R. Crane, A. J. Di Bilio, J. R. Winkler, H. B. Gray, *J. Am. Chem. Soc.* **2001**, *123*, 11623 – 11631.
[15] F. A. Tezcan, B. R. Crane, J. R. Winkler, H. B. Gray, *Proc. Natl. Acad. Sci. USA* **2001**, *98*, 5002 – 5006.
[16] S. A. Kang, B. R. Crane, *Proc. Natl. Acad. Sci. USA* **2005**, *102*, 15465 – 15470.
[17] T. Ueno, S. Abe, T. Koshiyama, T. Ohki, T. Hikage, Y. Watanabe, *Chem. Eur. J.* **2010**, *16*, 2730 – 2740.
[18] I. W. McNae, K. Fishburne, A. Habtemariam, T. M. Hunter, M. Melchart, F. Y. Wang, M. D. Walkinshaw, P. J. Sadler, *Chem. Commun.* **2004**, 1786 – 1787.
[19] A. Casini, G. Mastrobuoni, C. Temperini, C. Gabbiani, S. Francese, G. Moneti, C. T. Supuran, A. Scozzafava, L. Messori, *Chem. Commun.* **2007**, 156 – 158.
[20] T. Ni, F. A. Tezcan, *Angew. Chem.* **2010**, *122*, 7168 – 7172; *Angew. Chem. Int. Ed.* **2010**, *49*, 7014 – 7018.
[21] A. Cvetkovic, C. Picioreanu, A. J. J. Straathof, R. Krishna, L. A. M. van der Wielen, *J. Phys. Chem. B* **2005**, *109*, 10561 – 10566.
[22] Z. Q. Hu, J. W. Jiang, *J. Membr. Sci.* **2008**, *324*, 192 – 197.
[23] pymol, http://pymol.org/.
[24] T. Koshiyama, N. Kawaba, T. Hikage, M. Shirai, Y. Miura, C. Y. Huang, K. Tanaka, Y. Watanabe, T. Ueno, *Bioconjugate Chem.* **2010**, *21*, 264 – 269.
[25] M. Otake, M. Itou, Y. Araki, O. Ito, H. Kido, *Inorg. Chem.* **2005**, *44*, 8581 – 8586.
[26] K. Tsukahara, S. Asami, M. Okada, T. Sakurai, *Bull. Chem. Soc. Jpn.* **1994**, *67*, 421 – 431.
[27] K. Harada, M. Makino, H. Sugimoto, S. Hirota, T. Matsuo, Y. Shiro, Y. Hisaeda, T. Hayashi, *Biochemistry* **2007**, *46*, 9406 – 9416.
[28] S. Papp, J. M. Vanderkooi, C. S. Owen, G. R. Holtom, C. M. Phillips, *Biophys. J.* **1990**, *58*, 177 – 186.
[29] H. E. Toma, K. Araki, A. D. P. Alexiou, S. Nikolaou, S. Dovidauskas, *Coord. Chem. Rev.* **2001**, *219*, 187 – 234.
[30] B. Conlan, *Photosynth. Res.* **2008**, *98*, 687 – 700.
[31] C. Shih, A. K. Museth, M. Abrahamsson, A. M. Blanco-Rodriguez, A. J. Di Bilio, J. Sudhamsu, B. R. Crane, K. L. Ronayne, M. Towrie, A. Vlcek, J. H. Richards, J. R. Winkler, H. B. Gray, *Science* **2008**, *320*, 1760 – 1762.
[32] R. Langen, J. L. Colon, D. R. Casimiro, T. B. Karpishin, J. R. Winkler, H. B. Gray, *J. Biol. Inorg. Chem.* **1996**, *1*, 221 – 225.

